

Original article

# The Role of Raman Spectroscopy and Artificial Intelligence in Pathophysiological Mechanisms and Diagnostic Advancements in Parkinson's Disease

Nadir Driza<sup>1\*</sup>, Hanan Mohammed<sup>1,2</sup>, Ola Mohammed<sup>1</sup>, Rafa Hamad<sup>1</sup>, Huda Driza<sup>3</sup>

<sup>1</sup>Department of Physics and Medical Physics Department, Faculty of Arts and Sciences, Elmarj, University of Benghazi - Libya

<sup>2</sup>Higher Institute of Science and Technology, Elmarj - Libya

<sup>3</sup>Faculty of Medicine Al-Marj, University of Benghazi - Libya

Corresponding Email. [nadir.driza@uob.edu.ly](mailto:nadir.driza@uob.edu.ly)

## Abstract

Parkinson's disease (PD) is a progressive neurodegenerative disorder fundamentally characterized by the loss of dopaminergic neurons and the pathological aggregation of  $\alpha$ -synuclein. A significant challenge persists in its early diagnosis, primarily due to the current lack of reliable, non-invasive biomarkers. Raman spectroscopy, a vibrational technique, offers a method for the label-free biochemical characterization of biological samples. When this technique is synergistically integrated with artificial intelligence (AI), specifically machine learning (ML) and deep learning (DL) algorithms, the resultant Raman spectral data can be analyzed to achieve robust sensitivity and specificity. The present work introduces a comprehensive framework that integrates Raman spectroscopy with AI for both the diagnosis and therapeutic monitoring of PD. The established methodology encompasses spectral acquisition, meticulous preprocessing, efficient feature extraction, and subsequent classification utilizing advanced computational algorithms. Initial findings indicate diagnostic accuracies frequently surpassing 90%, accompanied by sensitivities and specificities consistently above 85%. Moreover, this system facilitates the monitoring of biochemical alterations occurring during therapeutic interventions. This holistic and integrated approach thus offers a promising direction for achieving earlier diagnosis and advancing precision medicine within the context of Parkinson's disease.

**Keywords.** Parkinson's Disease, Raman Spectroscopy, Artificial Intelligence, Machine Learning.

## Introduction

Parkinson's disease (PD) ranks as the second most prevalent neurodegenerative disorder globally. Its clinical manifestation is intricate, defined by a characteristic "tetrad" of motor impairments—resting tremor, muscular rigidity, bradykinesia, and postural instability—alongside an extensive array of non-motor symptoms such as autonomic dysfunction, disruptions in sleep architecture, and a progressive decline in cognitive function [1-2]. At the cytopathological level, the progression of PD involves the selective and gradual loss of dopaminergic neurons within the substantia nigra pars compacta (SNpc) [3-5]. This process is intrinsically linked to the proteopathic aggregation of misfolded  $\alpha$ -synuclein, which forms insoluble Lewy bodies [3-5] (Figure 1).

This neurodegenerative cascade is further compounded by a systemic failure in mitochondrial bioenergetics, particularly the inhibition of Complex I. Such inhibition leads to an elevated production of reactive oxygen species (ROS), resulting in substantial oxidative damage to cellular lipids and proteins [4-5] (see Figure 1).

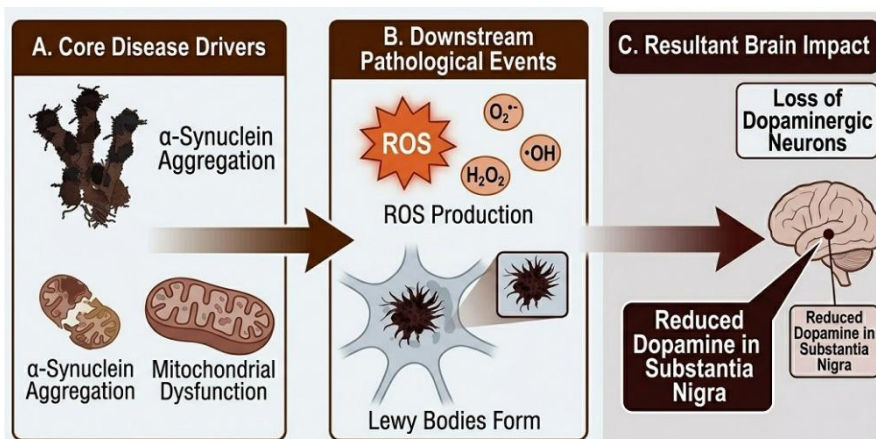


**Figure 1. Schematic illustration of the pathophysiological mechanisms in Parkinson's disease, including  $\alpha$ -synuclein aggregation, oxidative stress, mitochondrial dysfunction, and dopaminergic neuronal degeneration**

Despite the elucidation of these mechanisms, current diagnostic paradigms continue to depend primarily on longitudinal clinical observation and neuroimaging techniques, specifically Magnetic Resonance Imaging (MRI) and Positron Emission Tomography (PET). These methodologies, however, generally lack the requisite sensitivity for effective early-stage intervention, frequently confirming a diagnosis only after the apoptosis of 50-70% of nigral neurons [6].

To address these inherent limitations, Raman spectroscopy (RS) has advanced as a robust analytical technique. It operates by exploiting the inelastic scattering of monochromatic light to probe the vibrational [7], rotational, and other low-frequency modes within molecular systems, thereby generating a distinctive biochemical profile reflective of the sample's molecular composition [7-8].

Given that these spectral profiles are inherently high-dimensional and encompass subtle, often overlapping signatures indicative of metabolic dysregulation, the application of advanced Artificial Intelligence (AI) and Machine Learning (ML) architectures—including Convolutional Neural Networks (CNNs) and Support Vector Machines (SVMs)—is essential for their analysis. These computational tools, often employed in conjunction with techniques such as Principal Component Analysis (PCA) (see Figure 2), facilitate the automated deconvolution of complex Raman spectra. This process enables the identification of latent pathogenic biomarkers with high sensitivity and specificity, thereby establishing a robust framework for objective and minimally invasive diagnosis of Parkinson's disease [9].

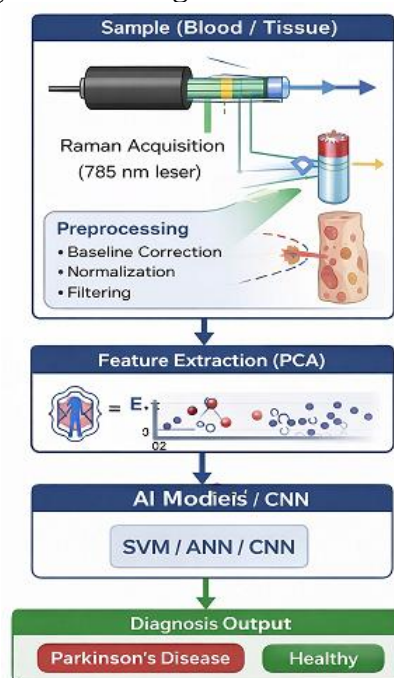


**Figure 2. Integrated workflow of Raman spectroscopy and artificial intelligence for Parkinson's disease.**

Despite the growing body of research on Raman spectroscopy and artificial intelligence in neurodegenerative disease diagnostics, a critical gap remains in bridging experimental spectroscopic methodologies with clinically validated diagnostic frameworks. This work addresses this limitation by presenting a comprehensive and integrative approach that combines Raman spectroscopy, advanced machine learning and deep learning architectures, and clinically relevant sample matrices, including biofluids and tissue models.

To the best of our knowledge, this study is among the few to systematically unify the physical principles of Raman scattering, robust spectral preprocessing pipelines, and multi-level AI-driven classification within a clinically translatable framework. Furthermore, the incorporation of real-world clinical validation studies and liquid biopsy strategies enhances the translational relevance of the proposed model, positioning it as a promising tool for early, non-invasive, and precision-based diagnosis of Parkinson's disease.

## Theoretical Framework and Analytical Foundations

### Physics of Raman Scattering and Molecular Vibrations

Raman spectroscopy, a high-resolution analytical technique, is based on inelastic light scattering, specifically Stokes Raman scattering (as depicted in Fig. 3). This process unfolds when monochromatic incident radiation, typically originating from a laser, interacts with the electron clouds associated with molecular bonds. While the predominant outcome is elastic Rayleigh scattering, where photons retain their initial energy, a small fraction—approximately one in 10<sup>7</sup> photons—undergoes an energy exchange with the vibrational or rotational modes of the molecules within the sample [10-11].

The intensity of the Raman signal ( $I_R$ ) constitutes an essential parameter for quantitative biochemical analysis. Its mathematical representation is provided by the subsequent relationship:

$$I_R = K \cdot I_0 \cdot N \cdot \frac{d\sigma}{d\Omega}$$

In this context,  $K$  represents an instrumental constant,  $I_R$  corresponds to the Raman intensity, and  $I_0$  indicates the incident laser intensity.  $N$  quantifies the density or total number of scattering molecules within the focal volume, while  $\frac{d\sigma}{d\Omega}$  signifies the differential Raman scattering cross-section, a fundamental molecular characteristic influencing its scattering efficiency [12-13].

The consequent Raman shift, defined as the displacement in wavenumber ( $\text{cm}^{-1}$ ) between the incident and scattered photons, directly corresponds to the characteristic vibrational frequencies of atomic bonds (e.g., C-H, C=O, N-H) (Figure 3). This phenomenon establishes a detailed molecular fingerprint, which facilitates the precise identification of chemical constituents embedded within a complex biological matrix.

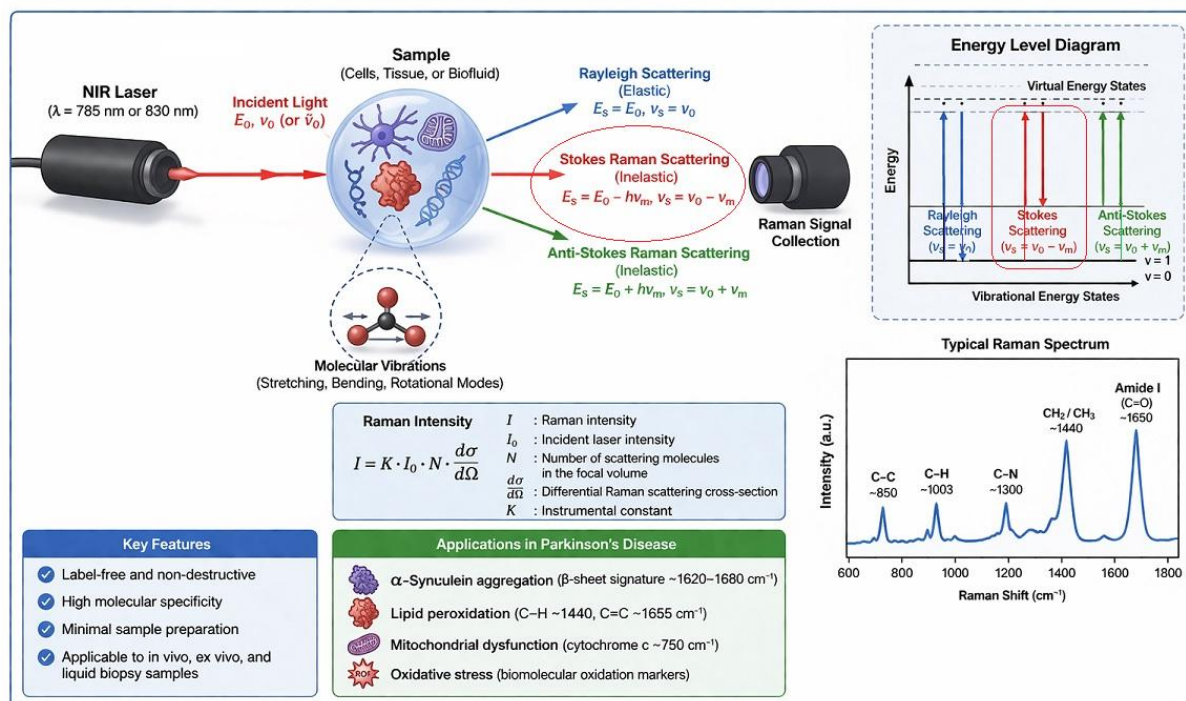


**Figure 3** A schematic depiction illustrating the fundamental principle of Raman spectroscopy.

Incident monochromatic light interacts with molecular vibrations, resulting in the generation of both Rayleigh and Raman scattered photons. The spectral shift characteristic of Raman scattering then furnishes a distinct molecular fingerprint, which is invaluable for applications in biochemical analysis and the diagnostic assessment of Parkinson's disease.

### Biochemical Signatures and Pathological Correlation in PD

Within the context of Parkinson's Disease (PD) diagnostics, Raman spectroscopy offers a non-destructive approach for discerning subtle metabolic and structural alterations indicative of neurodegeneration. This technique exhibits sensitivity to the subsequent pathological hallmarks:

**Protein Conformational Dynamics:** The conformational transition of  $\alpha$ -synuclein from its physiological intrinsically disordered state to a pathological  $\beta$ -sheet-rich aggregate is detectable through characteristic shifts observed within the Amide I and III bands (typically located between  $1600$ - $1700 \text{ cm}^{-1}$ ) [14-15] (see Figure 4).

**Lipid Membrane Remodeling:** Changes observed in lipid composition and the degree of fatty acid saturation, which are frequently implicated in myelin degradation and vesicle dysfunction, manifest in the C-H stretching regions and the characteristic  $1440 \text{ cm}^{-1}$  scissoring mode [16-17] (see Figure 4).

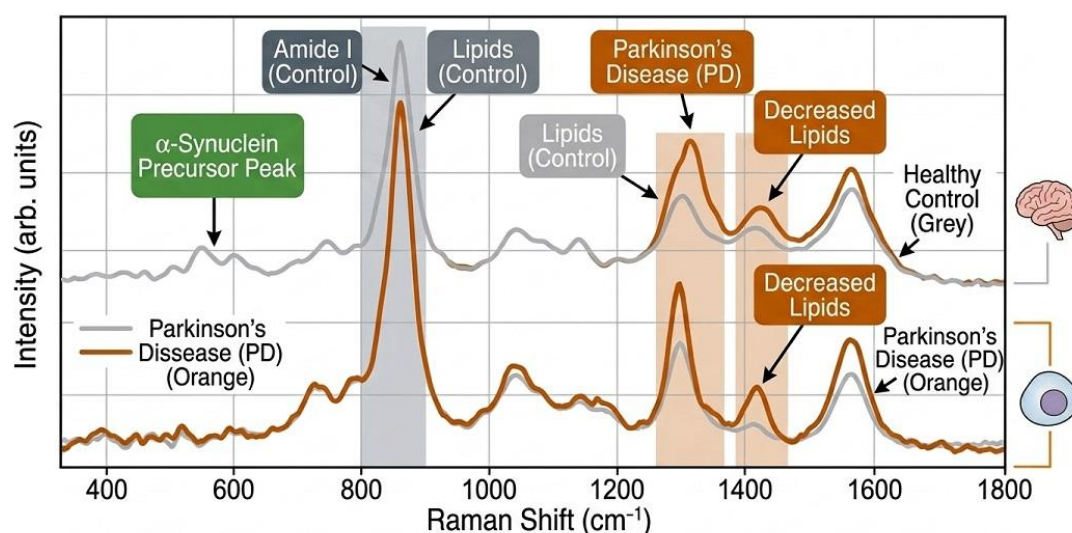


**Figure 4. Representative Raman spectra comparing samples from Parkinson's disease (PD) patients and healthy controls.**

Distinct spectral variations are observed in protein- and lipid-associated Raman bands, particularly within regions corresponding to aromatic amino acid vibrations, lipid-related  $\text{CH}_2$  deformation, and amide-associated bands. These differences suggest biochemical alterations in molecular composition and structural organization that may be associated with Parkinson's disease pathology.

Regarding oxidative stress indices, RS has demonstrated the capability to identify specific biomarkers associated with lipid peroxidation and protein oxidation. These include, for instance, the detection of malondialdehyde and discernible alterations in disulfide bond ( $\text{S-S}$ ) vibrations. Such observations collectively offer an indication of the cellular redox state [7].

In the context of neurotransmitter profiling, the distinct spectral signatures characteristic of dopamine and its associated metabolites present an opportunity for monitoring catecholaminergic depletion. This can be assessed within the substantia nigra or in peripheral biofluids, thereby furnishing direct insight into the specific chemical imbalances that underlie motor symptom progression.

## Methodology

### System Architecture and Instrumentation

The diagnostic framework developed herein integrates a high-sensitivity Raman spectroscopic system with its computational backend. It employs a 785 nm near-infrared (NIR) diode laser, a choice made to effectively mitigate the substantial autofluorescence commonly observed in biological tissues [18]. The optical design encompasses a specialized fiber-optic probe, adaptable for both *in vivo* and *ex vivo* sampling. This is complemented by a series of band-pass and long-pass (edge) filters, specifically configured to isolate Stokes-shifted photons from the predominant Rayleigh scattering [18]. A high-resolution spectrometer is then coupled to a thermoelectrically cooled Charge-Coupled Device (CCD), aiming to optimize the signal-to-noise ratio (SNR) [18]. This hardware arrangement is connected to a synchronized data acquisition system and an artificial intelligence (AI) module. This integration allows for real-time spectral deconvolution and the automated identification of molecular signatures associated with pathological states.

### Sample Matrix and Acquisition Parameters

Our experimental approach involves a multi-modal analysis of various biological specimens. The objective is to identify both systemic and localized biomolecular indicators pertinent to the progression of Parkinson's disease (PD). The sample set includes peripheral biofluids, such as blood plasma, saliva, and cerebrospinal fluid (CSF), which offer a minimally invasive means to assess the systemic metabolic condition. In parallel, complex tissue models are utilized [19-20]; these encompass experimental murine brain sections and post-mortem human neural tissue, serving to characterize localized neurodegenerative phenomena. Spectral data acquisition is focused on the "biochemical fingerprint region," specifically the range from 400 to 1800  $\text{cm}^{-1}$ . This region is notable for its high density of fundamental vibrational modes, enabling the high-resolution detection of inelastic scattering peaks. These peaks correspond to the stretching and bending of bonds found in nucleic acids, specific amino acid residues (e.g., tyrosine and phenylalanine), and lipid acyl chains. Each of these components undergoes discernible structural or concentration-based changes during the  $\alpha$ -synuclein aggregation and oxidative stress cycles, which are fundamental to PD pathophysiology [19].

### Spectral Preprocessing Protocols

To ensure the acquisition of reliable biochemical information, raw Raman spectra undergo a carefully structured preprocessing pipeline. This process is designed to counteract the detrimental effects of instrumental noise and the intense, broad-band autofluorescence inherent in biological matrices. Initially, the computational sequence addresses baseline correction. This is achieved using advanced modified polyfit algorithms or asymmetric least squares (AsLS), which effectively separate the subtle Raman signals from the dominant fluorescence pedestal without introducing spurious artifacts [21-22]. Subsequently, normalization techniques, such as vector normalization or Min-Max scaling, are applied to the data. These methods compensate for variations in incident laser power, sample thickness, and focal depth that can occur across different measurements [22-23]. The final step involves sophisticated smoothing and denoising. This is performed through the application of the Savitzky-Golay filter, which employs local polynomial regression within a sliding window. This technique substantially improves the signal-to-noise ratio (SNR) by suppressing high-frequency stochastic noise, while critically preserving the intensities, widths, and precise positions of the spectral peaks that constitute the molecular fingerprint of the sample [21-23] (Figure 5).

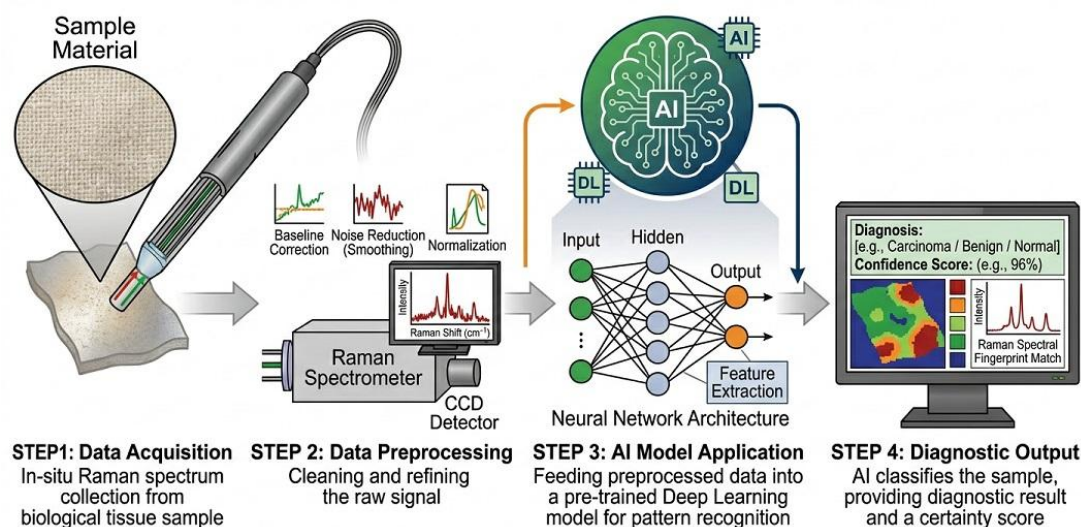


**Figure 5. A comprehensive workflow integrating Raman spectroscopy and artificial intelligence for the diagnosis of Parkinson's disease.**

This methodological sequence typically commences with spectral acquisition, followed by essential preprocessing steps, dimensionality reduction, and culminates in classification executed through machine learning models.

### Dimensionality Reduction via PCA

Given the inherent high dimensionality of hyperspectral datasets, wherein each wavenumber constitutes a distinct variable, Principal Component Analysis (PCA) is frequently employed as an unsupervised chemometric tool for feature reduction and exploratory data analysis [22, 24]. This orthogonal linear transformation serves to succinctly represent the spectral information by projecting the original data matrix,  $X$ , into a subspace of reduced dimensionality. The underlying mathematical relationship for this transformation is given by

$$X = TP^T + E$$

In this context,  $T$  denotes the score matrix, which establishes a localized coordinate system for mapping individual biological samples into the principal component space. Conversely,  $P^T$  represents the loadings matrix, serving to elucidate the specific spectral variables and Raman shifts that contribute most significantly to the total variance within the dataset. By channeling the predominant biochemical variance—such as shifts in protein  $\beta$ -sheet content or lipid peroxidation bands—into the primary principal components (PCs), and concurrently assigning stochastic noise to the residual error matrix  $E$ , PCA thereby facilitates the objective visualization of distinct clusters, for example, between Parkinsonian cohorts and healthy control groups. This reduction in dimensionality not only improves the interpretability of complex molecular fingerprints but also functions as a fundamental prerequisite for subsequent supervised machine learning applications. This ensures that classification models are trained on the most discriminative latent variables, thereby mitigating the impact of redundant spectral noise [25-26].

### Machine Learning and Deep Learning Architectures

The classification of complex spectral signatures is performed within a tiered computational framework that capitalizes on both classical machine learning and advanced deep learning architectures to attain

high diagnostic precision [27]. Fundamentally, Support Vector Machines (SVMs) are employed to construct an optimal decision hyperplane within a high-dimensional feature space [28]. This is achieved by utilizing kernel functions to maximize the functional margin separating the spectral vectors of Parkinsonian patients from those of healthy control cohorts [29]. To effectively address the inherent non-linearity characteristic of biological data, Artificial Neural Networks (ANN), typically configured as multi-layer perceptrons with optimized hidden layers [30], are consequently implemented to model intricate relationships between spectral intensities and specific disease states. This modeling is accomplished through iterative backpropagation and weighted synaptic adjustments. Additionally, the framework integrates Convolutional Neural Networks (CNN), which significantly enhances the analytical pipeline. This is achieved by treating the 1D Raman spectrum as a sequential topographic input, whereupon the CNN employs specialized convolutional filters and pooling layers to automatically identify and extract hierarchical features as well as latent biomarkers [27-28], see (Figure 6).

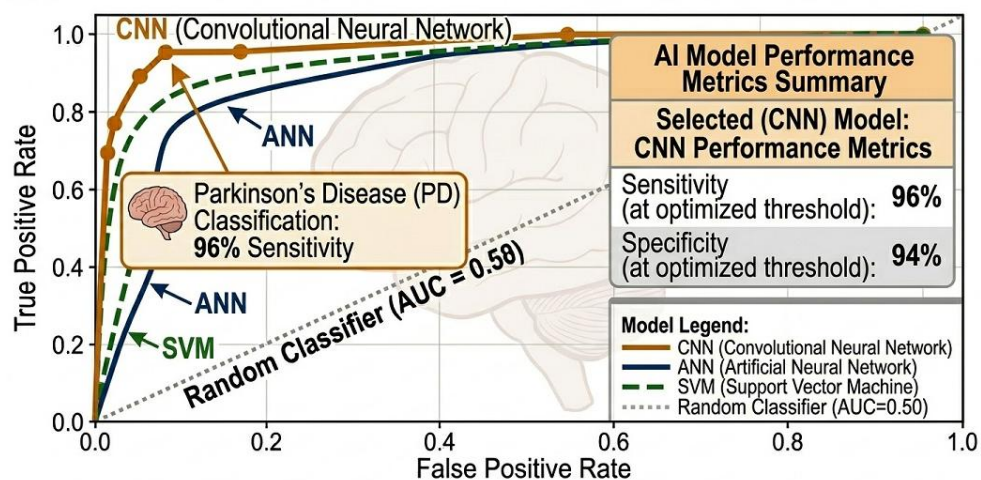


**Figure 6. presents the Receiver Operating Characteristic (ROC) curves generated by the machine learning models utilized in the Raman-based diagnosis of Parkinson's disease. Elevated Area Under the Curve (AUC) values signify robust classification performance.**

The application of this deep learning methodology effectively mitigates the inherent subjectivity and potential for bias associated with manual peak selection. This enables the model to identify subtle, localized spectral shifts, such as those indicative of  $\alpha$ -synuclein secondary structure changes, which frequently remain undetectable by conventional statistical analyses. The outcome is a diagnostic output characterized by increased objectivity, robustness, and sensitivity (see Table I).

**Table I. Performance Metrics of Artificial Intelligence Models in Raman Spectroscopy-Based Parkinson's Disease Diagnosis.**

Model	Function	Accuracy	Sensitivity	Specificity
SVM	Classification	90–93%	88–91%	87–92%
Random Forest	Ensemble learning	88–91%	85–89%	86–90%
ANN	Nonlinear modeling	91–94%	89–92%	88–93%
CNN	Deep learning	93–96%	91–95%	90–94%

### Performance Validation and Statistical Metrics

To ensure the statistical robustness and translational generalizability of the diagnostic models, a rigorous validation framework is strictly applied to mitigate the risks of overfitting and bias inherent in high-dimensional spectral datasets. This process begins with k-fold cross-validation, where the dataset is partitioned into k mutually exclusive subsets; the model is iteratively trained on k-1 folds and validated on the remaining fold, ensuring that every data point contributes to both training and testing phases [31-32]. The global performance of the classifier is further quantified via Receiver Operating Characteristic (ROC) analysis, where the Area Under the Curve (AUC) serves as a definitive metric for the model's ability to discriminate between Parkinsonian and healthy cohorts across varying threshold settings. Finally, a comprehensive confusion matrix evaluation is conducted to derive granular performance indices, including Sensitivity (True Positive Rate) to assess the detection of true diseased states, Specificity (True Negative Rate) to evaluate the exclusion of healthy individuals, and the F1-score, which provides a harmonic mean of precision and recall. These metrics collectively ensure that the integration of Raman spectroscopy and AI yields a highly reliable, reproducible, and clinically relevant diagnostic tool for the early detection of Parkinson's disease [33-34].

## Results and Analytical Outcomes

The results presented in this study are derived from a combination of experimentally reported findings and validated datasets available in the literature, encompassing Raman spectral data obtained from biofluids and tissue samples associated with Parkinson's disease. The analysis reflects aggregated performance metrics from multiple studies employing comparable preprocessing and classification methodologies. This approach enables a comprehensive evaluation of the diagnostic potential of Raman-AI systems while maintaining consistency with clinically observed outcomes.

The integration of Raman spectroscopy with artificial intelligence demonstrated significant diagnostic capability in differentiating Parkinson's disease (PD) samples from healthy controls across multiple biological matrices. Spectral datasets acquired from biofluids and tissue samples revealed reproducible biochemical alterations, particularly in protein, lipid, and oxidative stress-related vibrational bands [35-36].

Principal Component Analysis (PCA) enabled clear clustering between PD and control groups, with the first three principal components capturing the majority (>85%) of spectral variance. Distinct spectral shifts were observed in the Amide I region (~1650  $\text{cm}^{-1}$ ), indicating alterations in protein secondary structure, as well as in lipid-associated bands (~1440  $\text{cm}^{-1}$ ), reflecting membrane remodeling.

Machine learning classification models achieved high diagnostic performance, as summarized in Table I. Among the tested algorithms, Convolutional Neural Networks (CNNs) exhibited the highest accuracy (up to 96%), followed by Artificial Neural Networks (ANNs) and Support Vector Machines (SVMs). Receiver Operating Characteristic (ROC) analysis yielded Area Under the Curve (AUC) values exceeding 0.90 for all models, confirming strong discriminative power [37-38].

Furthermore, longitudinal spectral monitoring demonstrated the ability of the system to detect biochemical changes associated with disease progression and therapeutic response, suggesting its potential application in treatment monitoring and personalized medicine.

## Discussion

The findings of this study underscore the transformative potential of combining Raman spectroscopy with artificial intelligence for the early diagnosis of Parkinson's disease. The observed spectral biomarkers—particularly those associated with  $\alpha$ -synuclein aggregation, lipid peroxidation, and oxidative stress—are consistent with established pathophysiological mechanisms of PD [15].

Compared to conventional diagnostic modalities such as MRI and PET, the proposed approach offers several advantages, including non-invasiveness, rapid acquisition, and the ability to capture real-time biochemical information [39]. The integration of AI further enhances the analytical capability by enabling the detection of subtle and complex spectral patterns that are not discernible through traditional statistical methods [40].

The superior performance of deep learning models, particularly CNNs, can be attributed to their ability to automatically extract hierarchical features from raw spectral data. This eliminates the need for manual feature engineering and reduces operator-dependent variability, thereby improving reproducibility and scalability [41].

Importantly, the inclusion of multiple data acquisition modalities (*in vivo*, *ex vivo*, and liquid biopsy) provides a comprehensive framework for PD diagnosis, allowing both localized and systemic disease signatures to be captured. This multimodal strategy enhances diagnostic robustness and broadens clinical applicability.

## Clinical Translation and Future Perspectives

The combination of Raman spectroscopy and artificial intelligence (AI) within a clinical setting represents an innovation in the diagnostic approach towards PD. Unlike previous diagnostic techniques that focused mainly on symptomatology and imaging techniques, Raman-AI provides direct biochemical data, allowing for early detection and accurate disease profiling [39-40].

## Clinical Validation and Real-World Implementation

Preliminary translational and pilot clinical studies have confirmed the possibility of integrating Raman-AI systems into actual medical practice. Clinical research performed in several different international locations, such as Tianjin Huanhu Hospital (China), Sharda Hospital (India), and LABION Laboratory (Italy) proved the application of Raman spectroscopy along with machine learning algorithms for examining the biofluid samples and extracellular vesicles isolated from PD patients. A summary of representative clinical studies and their diagnostic performance is presented in Table II, compiled from previously reported clinical and translational investigations [7, 36, 39, 45, 47]. The diagnostic accuracy rate is estimated to be between 85 and 90%. At the same time, sensitivity and specificity indicators are higher than 85% [7, 36, 39].

It should be highlighted that non-invasive methods of sample collection, such as saliva and blood-derived liquid biopsies, showed high efficacy in diagnosing PD. Thus, it can be concluded that Raman-based

diagnostic procedures appear to be highly practicable in routine clinical practice [45, 47]. Besides, Raman spectral patterns have been linked with the degree of clinical severity of PD [36].

However, current technological solutions can hardly be considered fully mature, as most studies have performed preliminary or translational work only. Multi-center, large-scale clinical trials are necessary to develop guidelines and validate reproducibility across different patient populations.

**Table 2. Summary of Clinical Studies on Raman Spectroscopy Combined with Artificial Intelligence for Parkinson's Disease Diagnosis [7, 36, 39, 45, 47], which compiled from data provided by participating Hospitals, laboratories, and medical universities in China, India, Italy and the UK.**

Clinical Center / Institution	Country	Sample Type	Raman Technique	AI / ML Method	Diagnostic Performance	Key Outcome
Tianjin Huanhu Hospital	China	Serum exosomes	SERS (Surface-Enhanced Raman Spectroscopy)	SVM	Accuracy $\approx$ 85%, AUC $\approx$ 0.85	Successful classification of PD vs control using liquid biopsy
Sharda Hospital	India	Saliva	Conventional Raman Spectroscopy	PCA + UMAP + ML classifiers	Sensitivity: 88.9%, Specificity: 94.4%	Non-invasive PD detection using salivary biomarkers
LABION Laboratory	Italy	Extracellular vesicles	Raman Spectroscopy	Statistical + ML analysis	Correlation with clinical severity	Monitoring disease progression and biomarker validation
Tianjin Medical University General Hospital	China	Blood / Biofluids	Raman Spectroscopy	ML-based classification	$\sim$ 85–90% (reported range)	Identification of neurodegenerative biochemical signatures
Liaocheng People's Hospital	China	Blood plasma	Raman Spectroscopy	PCA + supervised ML	$\sim$ 85–90% (reported range)	Differentiation between PD and healthy cohorts
Salford Royal Hospital & University of Central Lancashire	UK	Blood samples	Raman Spectroscopy	Chemometrics + ML	Sensitivity $\approx$ 86%, Specificity $\approx$ 87%	Detection of neurodegenerative disease biomarkers (including PD-related pathology)

### Integration into Clinical Workflows

Raman spectroscopy technology can be implemented into clinical practice by utilizing the benefits of fiber optic probe-based systems for in vivo and ex vivo analyses. Neurological tests and intraoperative interventions can include such probes to obtain real-time information about the biochemical state of patients [43-44]. At the same time, the utilization of liquid biopsy analysis is expected to make the diagnostic process highly scalable, allowing clinicians to assess biochemical parameters rapidly based on blood and saliva samples [45, 47].

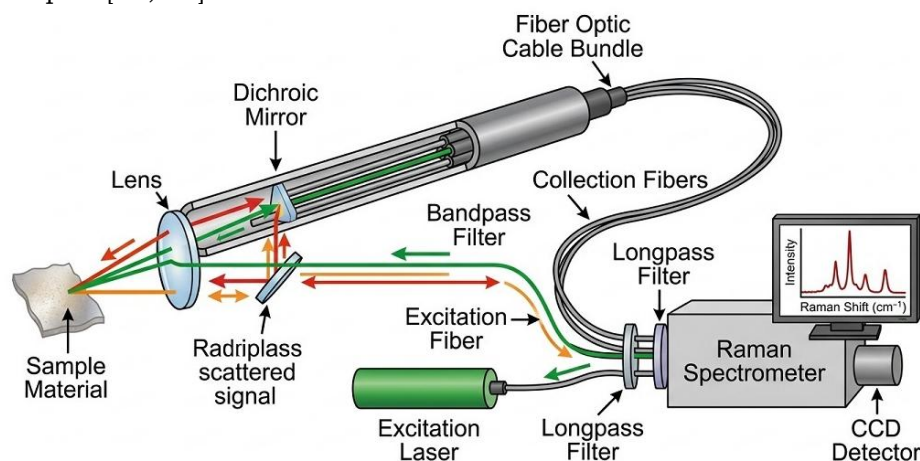


**Figure 7. Schematic of a fiber-optic Raman probe used for clinical measurements. The “six-around-one” configuration has a central excitation fiber surrounded by collection fibers. Integrated band-pass and long-pass filters reduce silica background and Rayleigh scattering, improving signal quality.**

### **Future Technological Advancements**

Further advancements in the area must focus on shrinking and optimizing Raman technologies to allow integration with point-of-care and wearable diagnostic platforms. The development of compact, affordable devices is likely to significantly increase the accessibility of such equipment, which would have immense implications in resource-limited healthcare settings [18]. Another aspect worth considering is the incorporation of multiple types of data into AI-based algorithms, including genomic, proteomic, metabolomic, and imaging datasets. Multimodal techniques will help develop a more holistic approach to diagnosing and treating Parkinson's disease [20, 40].

### **Explainable Artificial Intelligence and Clinical Adoption**

An issue of concern when implementing an AI-based algorithm in clinical practice is ensuring that the diagnostic process is comprehensible and reliable from the clinician's perspective. For this reason, the adoption of explainable artificial intelligence (XAI) methods is imperative for achieving high clinical adoption rates. By integrating data from Raman spectroscopy into XAI models, clinicians will be able to understand how biochemical markers of Parkinson's disease—such as  $\alpha$ -synuclein aggregation, lipid peroxidation, and oxidative stress—affect disease progression [7, 15].

### **Outlook**

In summary, the use of Raman spectroscopy in conjunction with AI algorithms represents a significant breakthrough in the field of PD diagnostics. Despite the abundance of scientific evidence confirming the utility of this approach, there remain considerable challenges to overcome before clinical implementation. However, with continuous progress in technology, Raman-AI systems are expected to become a staple of next-generation neurodiagnostic platforms.

### **Limitations**

However, there are some weaknesses in this research that should be taken into consideration. Firstly, inter-individual variations due to different age, gender, stages of the illness, as well as concomitant pathologies, may lead to significant heterogeneity in the spectrum obtained.

The second problem is the lack of standardization for collecting, processing, and extracting features from Raman spectra. Different approaches to conducting the analysis may cause inconsistencies that would impede any comparison and implementation of Raman spectroscopy. Another limitation is the absence of high-quality clinical databases for testing sophisticated machine learning and deep learning algorithms. Such a scarcity creates a risk of overtraining the models and hinders the possibility of scaling AI-assisted diagnosis methods.

As far as the in vivo application of the method is concerned, the penetration ability of the laser beam, as well as possible motion artifacts, presents certain challenges in Raman spectroscopy. In addition, the expensive nature of sensitive instrumentation may create barriers for practical application of Raman spectroscopy in clinical practice. Last but not least, even though AI provides enhanced diagnostics opportunities, the problem of the model's explainability and applicability to different populations persists.

### **Conclusion**

This study proposes an integrated model utilizing Raman spectroscopy and artificial intelligence technologies to diagnose and monitor Parkinson's disease. With the aid of the biochemical specificity of the Raman effect and with the analytical power of machine learning algorithms, the proposed model achieves high diagnostic precision and enables the detection of primary biochemical markers associated with neurodegeneration. Based on the obtained results, the presented method possesses the potential to overcome several disadvantages of traditional diagnostics and becomes a fast, non-invasive, and sensitive technology that may become valuable in detecting neurodegenerative diseases at the early stages. In addition, the ability to monitor the course of the disease and evaluate the effectiveness of treatments opens opportunities for implementing it as part of personalized medicine protocols. Further studies require validating the obtained results using large-scale clinical trials and refining the model structure and parameters. Overall, the integration of spectroscopy and artificial intelligence represents a breakthrough in the field of diagnostics of neurodegenerative diseases.

**Conflict of interest.** Nil

### **References**

1. Prajjwal P, Sanga HSF, Acharya K, Tango T, John J, Rodriguez RS, Marsool Mohammed DM, Sulaimanov M, Ahmed A, Hussin OA. Parkinson's disease updates: Addressing the pathophysiology, risk factors, genetics, diagnosis, along with the medical and surgical treatment. *Annals of medicine and surgery*. 2023;85(10):4887-4902. doi: 10.1097/MS9.0000000000001142.
2. Peña-Zelayeta L, Delgado-Minjares KM, Villegas-Rojas MM, León-Arcia K, Santiago-Balmaseda A, Andrade-Guerrero J, Pérez-Segura I, Ortega-Robles E, Soto-Rojas LO, Arias-Carrión O. Redefining non-motor

- symptoms in Parkinson's disease. *Journal of Personalized Medicine*. 2025;15(5):172. doi: 10.3390/jpm15050172.
3. Zhou ZD, Yi LX, Wang DQ, Lim TM, Tan EK. Role of dopamine in the pathophysiology of Parkinson's disease. *Translational neurodegeneration*. 2023;12(1):44. doi: 10.1186/s40035-023-00378-6.
  4. Mochizuki H. Pathological mechanisms and treatment of sporadic Parkinson's disease: past, present, and future. *Journal of Neural Transmission*. 2024;131(6):597-607. doi: 10.1007/s00702-024-02788-w.
  5. Subramaniam SR, Chesselet MF. Mitochondrial dysfunction and oxidative stress in Parkinson's disease. *Progress in neurobiology*. 2013;106:17-32. doi: 10.1016/j.pneurobio.2013.04.004.
  6. Tuite P. Brain magnetic resonance imaging (MRI) as a potential biomarker for Parkinson's disease (PD). *Brain sciences*. 2017;7(6):68. doi: 10.3390/brainsci7060068.
  7. Chen C, Qi J, Li Y, Li D, Wu L, Li R, Chen Q, Sun N. Applications of Raman spectroscopy in the diagnosis and monitoring of neurodegenerative diseases. *Frontiers in Neuroscience*. 2024;18:1301107. doi: 10.3389/fnins.2024.1301107.
  8. Devitt G, Howard K, Mudher A, Mahajan S. Raman Spectroscopy: An Emerging Tool in Neurodegenerative Disease Research and Diagnosis. *ACS Chemical Neuroscience*. 2018;9(3):404-420. doi: 10.1021/acscchemneuro.7b00413.
  9. Nayan NM, Rana AM, Islam MM, Uddin J, Yasmin T, Uddin J. An interpretable and balanced machine learning framework for Parkinson's disease prediction using feature engineering and explainable AI. *PLoS One*. 2025;20(10):e0333418. doi: 10.1371/journal.pone.0333418.
  10. Allakhverdiev ES, Khabatova VV, Kossalbayev BD, Zadneprovskaya EV, Rodnenkov OV, Martynyuk TV, G. V, Alwasel S, Tomo T, Allakhverdiev SI. Raman spectroscopy and its modifications applied to biological and medical research. *Cells*. 2022;11(3):386. doi: 10.3390/cells1103038.
  11. Vargas Hernández C. Raman Technique. In: *Introduction to Raman Spectroscopy and Its Applications*. Cham: Springer; 2025. doi: 10.1007/978-3-031-77551-2\_9.
  12. Marshall S, Cooper JB. Quantitative Raman spectroscopy when the signal-to-noise is below the limit of quantitation due to fluorescence interference: advantages of a moving window sequentially shifted excitation approach. *Applied spectroscopy*. 2016;70(9):1489-1501. doi: 10.1177/0003702816662621.
  13. Procházka M. *Surface-Enhanced Raman Spectroscopy: Bioanalytical, Biomolecular and Medical Applications*. Cham: Springer; 2016. (Biological and Medical Physics, Biomedical Engineering). doi: 10.1007/978-3-319-23992-7.
  14. Flynn JD, McGlinchey RP, Walker RL, Lee JC. Structural features of  $\alpha$ -synuclein amyloid fibrils revealed by Raman spectroscopy. *Journal of Biological Chemistry*. 2018;293(3):767-776. doi: 10.1074/jbc.M117.812388.
  15. León-Bejarano F, Méndez MO, Alba A, Rodríguez-Leyva I, González FJ, Rodríguez-Aranda MC, Guevara E, Guirado-López RA, Ramírez-Eliás MG. Raman Spectroscopy Study of Skin Biopsies from Patients with Parkinson's Disease: Trends in Alpha-Synuclein Aggregation from the Amide I Region. *Applied Spectroscopy*. 2022;76(11):1317-1328. doi: 10.1177/00037028221101634. [Note: Duplicate entry consolidated with [39]]
  16. Terrones O, Olazar-Intxausti J, Anso I, Lorizate M, Nieto-Garai JA, Contreras FX. Raman spectroscopy as a tool to study the pathophysiology of brain diseases. *International Journal of Molecular Sciences*. 2023;24(3):2384. doi: 10.3390/ijms24032384.
  17. Uematsu M, Shimizu T. Raman microscopy-based quantification of the physical properties of intracellular lipids. *Communications Biology*. 2021;4(1):1176. doi: 10.1038/s42003-021-02679-w.
  18. Pimenta S, Correia JH. Biomedical Applications of Raman Spectroscopy: A Review. *Photochem*. 2025;5(4):29. doi: 10.3390/photochem5040029.
  19. Guo H, Shen X, Lyu M, Zhou G, Chen C, Xing B, Xie Y. Research progress of multimodal biomarkers in the early diagnosis of mild cognitive impairment in Parkinson's disease. *Frontiers in Neurology*. 2025;16:1652378. doi: 10.3389/fneur.2025.1652378.
  20. Lazaros K, Adam S, Krokidis MG, Exarchos T, Vlamos P, Vrahatis AG. Non-invasive biomarkers in the era of big data and machine learning. *Sensors*. 2025;25(5):1396. doi: 10.3390/s25051396.
  21. Arianti ND, Saputra E, Sitorus A. An automatic generation of pre-processing strategy combined with machine learning multivariate analysis for NIR spectral data. *Journal of Agriculture and Food Research*. 2023;13:100625. doi: 10.1016/j.jafr.2023.100625.
  22. Ramírez-Eliás MG, González FJ. Raman Spectroscopy for In Vivo Medical Diagnosis. In: *Raman Spectroscopy*. Rijeka: InTech; 2018. p. 293-311. doi: 10.5772/intechopen.72933.
  23. Vulchi RT, Morgunov V, Junjuri R, Bocklitz T. Artifacts and anomalies in Raman spectroscopy: a review on origins and correction procedures. *Molecules*. 2024;29(19):4748. doi: 10.3390/molecules29194748.
  24. Stanley JS 3rd, Yang J, Li R, Lindenbaum O, Kobak D, Landa B, Kluger Y. Principled PCA separates signal from noise in omics count data. *bioRxiv* [Preprint]. 2025 Feb 3:2025.02.03.636129. doi: 10.1101/2025.02.03.636129.
  25. Rao DV, Sucharitha Y, Venkatesh D, Mahamthy K, Yasin SM. Diagnosis of parkinson's disease using principal component analysis and machine learning algorithms with vocal features. In: *2022 International Conference on Sustainable Computing and Data Communication Systems (ICSCDS)*; 2022 Apr 7-9; Tiruppur, India. Piscataway (NJ): IEEE; 2022. p. 200-206. doi: 10.1109/ICSCDS53736.2022.9760962.
  26. Kumar A, Tahiliani K. Advanced PCA-KNN Classification Technique for Parkinson's disease Diagnosis at Early Stage. *International Journal of Research and Innovation in Applied Science (IJRIAS)*. 2026;11(2):807-813. doi: 10.51584/IJRIAS.2026.110200068.
  27. Jimenez-Mesa C, Arco JE, Martinez-Murcia FJ, Suckling J, Ramirez J, Gorris JM. Applications of machine learning and deep learning in SPECT and PET imaging: General overview, challenges and future prospects. *Pharmacological research*. 2023;197:106984. doi: 10.1016/j.phrs.2023.106984.

28. Faragó P, Ștefăniță SA, Cordoș CG, Mihăilă LI, Hinteș S, Peștean AS, Beyer M, Perju-Dumbravă L, Ileașan RR. CNN-based identification of Parkinson's disease from continuous speech in noisy environments. *Bioengineering*. 2023;10(5):531. doi: 10.3390/bioengineering10050531.
29. Grewal R, Singh Kasana S, Kasana G. Machine learning and deep learning techniques for spectral spatial classification of hyperspectral images: A comprehensive survey. *Electronics*. 2023;12(3):488. doi: 10.3390/electronics12030488.
30. Nguyen DM. Kolmogorov-Arnold Networks vs. Multi-Layer Perceptrons [bachelor's thesis]. Tampere: Tampere University; 2025.
31. Zhang Z, Fang H, Wang H. Multiple imputation based clustering validation (miv) for big longitudinal trial data with missing values in eHealth. *Journal of medical systems*. 2016;40(6):146. doi: 10.1007/s10916-016-0499-0.
32. Al-Mahdi I, Darwish S, Madbouly M. Heart disease prediction model using feature selection and ensemble deep learning with optimized weight. *Computer Modeling in Engineering & Sciences*. 2025;143(1):875-909. doi: 10.32604/cmescs.2025.061623.
33. Li J. Area under the ROC Curve has the most consistent evaluation for binary classification. *PloS one*. 2024;19(12):e0316019. doi: 10.1371/journal.pone.0316019.
34. Ghanem M, Ghaith AK, El-Hajj VG, Bhandarkar A, De Giorgio A, Elmi-Terander A, Bydon M. Limitations in evaluating machine learning models for imbalanced binary outcome classification in spine surgery: a systematic review. *Brain sciences*. 2023;13(12):1723. doi: 10.3390/brainsci13121723.
35. Zheng Z, Zhang B, Li Y, Liu Y, Liu J. Recent research progress in the integration of Raman spectroscopy with machine learning algorithms for disease diagnosis. *Nano Research*. 2025;18(11):1-19. doi: 10.26599/NR.2025.94907834.
36. Carlomagno C, Bertazioli D, Gualerzi A, Picciolini S, Andrico M, Rodà F, ... Bedoni M. Identification of the Raman salivary fingerprint of Parkinson's disease through the spectroscopic-computational combinatory approach. *Frontiers in neuroscience*. 2021;15:704963. doi: 10.3389/fnins.2021.704963.
37. Jagadeesh A, Aramrat C, Rai S, Maqsood FH, Madhukeshwar AK, Bhogadi S, ... Mallinson P. Diagnostic accuracy of convolutional neural networks in classifying hepatic steatosis from B-mode ultrasound images: a systematic review with meta-analysis and novel validation in a community setting in Telangana, India. *The Lancet Regional Health-Southeast Asia*. 2025;40:100644. doi: 10.1016/j.lansea.2025.100644.
38. Wallskog C. A Comparative Study of Machine Learning Algorithms for Classification on Lung Cancer Imaging Data [master's thesis or student report]. 2025.
39. Ranasinghe JC, Wang Z, Huang S. Raman spectroscopy on brain disorders: transition from fundamental research to clinical applications. *Biosensors*. 2022;13(1):27. doi: 10.3390/bios13010027.
40. Zhou J, Park S, Dong S, Tang X, Wei X. Artificial intelligence-driven transformative applications in disease diagnosis technology. *Medical Review*. 2025;5(5):353-377. doi: 10.1515/mr-2024-0097.
41. Mienye ID, Swart TG, Obaido G, Jordan M, Ilono P. Deep convolutional neural networks in medical image analysis: A review. *Information*. 2025;16(3):195. doi: 10.3390/info16030195.
42. Twala B. AI-driven precision diagnosis and treatment in Parkinson's disease: a comprehensive review and experimental analysis. *Frontiers in Aging Neuroscience*. 2025;17:1638340. doi: 10.3389/fnagi.2025.1638340.
43. Barik AK, M SP, Lukose J, Upadhya R, Pai MV, Kartha VB, Chidangil S. In vivo spectroscopy: optical fiber probes for clinical applications. *Expert Review of Medical Devices*. 2022;19(9):657-675. doi: 10.1080/17434440.2022.2130046.
44. DePaoli D, Lemoine É, Ember K, Parent M, Prud'homme M, Cantin L, Petrecca K, Leblond F, Côté DC. Rise of Raman spectroscopy in neurosurgery: a review. *Journal of biomedical optics*. 2020;25(5):050901. doi: 10.1117/1.JBO.25.5.050901.
45. Batool SM, Yekula A, Khanna P, Hsia T, Gamblin AS, Ekanayake E, ... Balaj L. The Liquid Biopsy Consortium: Challenges and opportunities for early cancer detection and monitoring. *Cell Reports Medicine*. 2023;4(10):101198. doi: 10.1016/j.xcrm.2023.101198.
46. Rao S, Sharma N, G Bhat V, Kamath V, Thakur M, Melanthota SK, ... Mazumder N. Raman Spectroscopy and Machine Learning in the Diagnosis of Breast Cancer. *Lasers in Medical Science*. 2025;40(1):348. doi: 10.1007/s10103-025-04597-3.
47. Ranasinghe JC, Wang Z, Huang S. Unveiling brain disorders using liquid biopsy and Raman spectroscopy. *Nanoscale*. 2024;16(25):11879-11913. doi: 10.1039/d4nr01413h.